



# CHORUS

This is the accepted manuscript made available via CHORUS. The article has been published as:

## Chiral Higgs Mode in Nematic Superconductors

Hiroki Uematsu, Takeshi Mizushima, Atsushi Tsuruta, Satoshi Fujimoto, and J. A. Sauls

Phys. Rev. Lett. **123**, 237001 — Published 3 December 2019

DOI: [10.1103/PhysRevLett.123.237001](https://doi.org/10.1103/PhysRevLett.123.237001)

# Chiral Higgs Mode in Nematic Superconductors

Hiroki Uematsu,<sup>1</sup> Takeshi Mizushima,<sup>1,\*</sup> Atsushi Tsuruta,<sup>1</sup> Satoshi Fujimoto,<sup>1</sup> and J. A. Sauls<sup>2</sup>

<sup>1</sup>Department of Materials Engineering Science, Osaka University, Toyonaka, Osaka 560-8531, Japan

<sup>2</sup>Center for Applied Physics & Superconducting Technologies  
Department of Physics, Northwestern University, Evanston, IL 60208 USA

(Dated: November 11, 2019)

Nematic superconductivity with spontaneously broken rotation symmetry has recently been reported in doped topological insulators,  $M_x\text{Bi}_2\text{Se}_3$  ( $M=\text{Cu, Sr, Nb}$ ). Here we show that the electromagnetic (EM) response of these compounds provides a spectroscopy for bosonic excitations that reflect the pairing channel and the broken symmetries of the ground state. Using quasiclassical Keldysh theory, we find two characteristic bosonic modes in nematic superconductors: the nematicity mode and the chiral Higgs mode. The former corresponds to the vibrations of the nematic order parameter associated with broken crystal symmetry, while the latter represents the excitation of chiral Cooper pairs. The chiral Higgs mode softens at a critical doping, signaling a dynamical instability of the nematic state towards a new chiral ground state with broken time reversal and mirror symmetry. Evolution of the bosonic spectrum is directly captured by EM power absorption spectra. We also discuss contributions to the bosonic spectrum from sub-dominant pairing channels to the EM response.

*Introduction.* Spontaneous symmetry breaking is an important concept that spreads across the diverse fields of modern physics. The recent discovery of two-fold rotation symmetry in superconducting compounds,  $M_x\text{Bi}_2\text{Se}_3$  ( $M = \text{Cu, Sr, Nb}$ ), has stimulated an intense discussion of superconductivity with a new class of spontaneous symmetry breaking [1–11]. The rotation symmetry breaking in the basal plane is compatible with odd-parity time-reversal invariant pairing belonging to the two-dimensional irreducible representation ( $E_u$ ) of the  $D_{3d}$  symmetry, which exhibits twofold symmetric gap anisotropy (Fig. 1). The anisotropy is represented by a nematic order parameter [12]. The odd-parity superconductor (SC)  $M_x\text{Bi}_2\text{Se}_3$  has also attracted much attention as a prototype of DIII topological SCs that host helical Majorana fermions [13–21]. In addition, there exist competing pairing channels corresponding to the  $A_{1g}$ ,  $A_{1u}$ , and  $A_{2u}$  irreducible representations, in addition to the “nematic”  $E_u$  state [14].

In this Letter, we report theoretical results showing that the electromagnetic (EM) response at microwave frequencies provides a spectroscopy for long-lived bosonic excitations that are “fingerprints” of the nematic ground state that breaks the maximal symmetry  $G = D_{3d} \times T \times U(1)_N$  of the parent compound down to  $H = C_{2v} \times T$ , where  $T$ ,  $U(1)_N$ , and  $D_{3d}$  and  $C_{2v}$  denote time-reversal symmetry, global gauge symmetry, and point-groups for three- and two-fold rotations, respectively [22]. We first discuss the Fermi-surface evolution that drives the nematic-to-chiral phase transition within the  $E_u$  representation. Using the quasiclassical Keldysh theory, we find two characteristic bosonic modes in nematic SCs: the nematicity mode and the chiral Higgs mode. The former corresponding to transverse oscillations of the nematic order parameter is the pseudo-Nambu-Goldstone (NG) boson associated with the broken  $D_{3d}$  symmetry. The latter represents the excitation of chiral Cooper pairs. We find that the mass gap of the chiral mode tends to zero as the Fermi surface changes topology from a closed spherical shape to an open cylindrical Fermi surface, signaling the dynamical instability of the nematic state towards the chiral state with broken time-reversal and mirror symmetries. Bosonic modes of unconventional SCs involve the coherent dynamics of macroscopic fractions of electrons, and reflect the broken symmetries and

the sub-dominant pairing interactions [23–37]. The bosonic excitation spectrum can be detected through transverse EM wave absorption [see Fig. 1(a)]. We also consider bosonic modes corresponding to the sub-dominant odd-parity  $A_{1u}$  and  $A_{2u}$  representations.

*Effective Hamiltonian.* Electrons embedded in  $M_x\text{Bi}_2\text{Se}_3$  exhibit (i) the orbital degrees of freedom, (ii) strong spin-orbit coupling, and (iii) evolution of the Fermi surface with increase in carrier concentration (see Fig. 1) [38, 39]. The low-energy physics is governed by electrons in two  $p_z$ -orbitals near the Fermi level. The effective Hamiltonian is given as [40–43]

$$\xi(\mathbf{p}) = c(\mathbf{p}) + m(\mathbf{p})\sigma_x + v_z f_z(p_z)\sigma_y + v(\mathbf{p} \times \mathbf{s})_z \sigma_z - \mu, \quad (1)$$

where  $c(\mathbf{p}) = c_0 + c_1 f_\perp(\mathbf{p}) + c_2 p_\parallel^2$ ,  $m(\mathbf{p}) = m_0 + m_1 f_\perp(\mathbf{p}) + m_2 p_\parallel^2$ , and  $\mu$  are the diagonal self-energy correction, band gap, and the chemical potential, respectively ( $p_\parallel^2 \equiv p_x^2 + p_y^2$ ). Nearest-neighbor hopping along the  $z$  direction gives  $f_z(p_z) = \frac{1}{c} \sin(p_z c)$  and  $f_\perp = \frac{2}{c^2} [1 - \cos(p_z c)]$ . We take the  $\hat{z}$  axis along the (111) direction of the crystal, and  $\mathbf{s}$  ( $\boldsymbol{\sigma}$ ) is the spin (orbital) Pauli matrices. The Hamiltonian in Eq. (1) maintains the enlarged  $D_\infty$  symmetry including  $SO(2)$  about the  $z$ -axis, while a higher order correction on  $p$  introduces three mirror planes and threefold rotational symmetry in the  $xy$  plane [12].

The intercalation of  $M$  atoms increases the carrier concentration in the conduction band (CB). As  $\mu \gg \Delta$  in typical materials (where  $\Delta$  is the superconducting gap), low-energy properties of the superconducting states are governed by the CB electrons with the dispersion  $E_{CB}(\mathbf{p}) = c - \mu + \sqrt{m^2 + v_z^2 f_z^2 + v^2 p_\parallel^2}$ , which is well separated from the valence band by the band gap,  $|m_0| \sim \mu$ , at the  $\Gamma$  point. Hence, we focus on the Hamiltonian for CB electrons interacting through the odd-parity pairing interaction within  $D_{3d} \times T \times U(1)_N$ ,

$$V_{\mu\nu}(\mathbf{p}, \mathbf{p}') = - \sum_{\Gamma} \sum_{i=1}^{n_\Gamma} V_i^{(\Gamma)} d_{\mu,i}^\Gamma(\mathbf{p}) d_{\nu,i}^{\Gamma*}(\mathbf{p}'). \quad (2)$$

where  $\Gamma = A_{1u}, A_{2u}$ , and  $E_u$  are the odd-parity irreducible representations of  $D_{3d}$  with the dimension  $n_\Gamma$  and basis functions  $\{d_1^\Gamma, \dots, d_{n_\Gamma}^\Gamma\}$ . The basis functions in lowest order in  $p$  are  $d_1^{E_u} =$

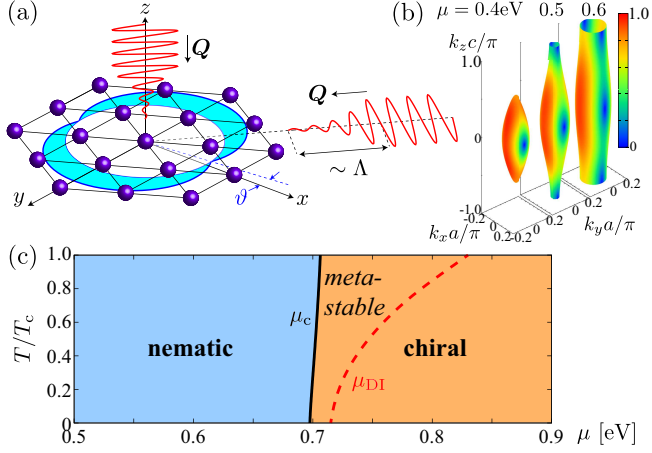


FIG. 1. (a) Configurations of polarized EM waves to probe the nematic pairing gap in the  $D_{3d}$  crystal structure. (b) Evolution of the Fermi surface and superconducting gap in the nematic state for various  $\mu$ . (c) Phase diagram of  $M_x\text{Bi}_2\text{Se}_3$  computed by the quasiclassical theory with  $\eta_1 = \Delta(T, \mu)$  and  $\eta_2 = 0$ . We set  $T_c^{(E_u, 2)} = T_c$  with  $T_c \equiv T_c^{(E_u, 1)}$ . The dashed curve shows the dynamical instability of the chiral Higgs mode beyond which the nematic state is no longer metastable.

$(v_z f_z / |m_0|, 0, -v p_x / m_0)$ ,  $\mathbf{d}_2^{E_u} = (0, v_z f_z / |m_0|, -v p_y / m_0)$ ,  $\mathbf{d}_1^{A_{1u}} = (v p_x / |m_0|, v p_y / |m_0|, v f_z(\mathbf{p}) / m_0)$ , and  $\mathbf{d}_1^{A_{2u}} = (-v p_y, v p_x, 0) / |m_0|$ . In the following we utilize the more general form of  $\mathbf{d}_i^\Gamma$  [44]. By employing the regularization of gap equations, the pairing interaction of the  $(\Gamma, i)$  channel,  $V_i^{(\Gamma)}$ , can be related to the instability temperature of the  $(\Gamma, i)$  gap function,  $T_c^{(\Gamma, i)}$  [44]. We set  $T_c \equiv T_c^{(E_u, 1)}$ .

*Nematic-to-chiral phase transition.* We consider the ground state within the  $E_u$  representation, i.e.,  $T_c \geq T_c^{(E_u, 2)} > T_c^{(A_{1u})}, T_c^{(A_{2u})}$ , where the equilibrium odd-parity  $E_u$  order parameter in the CB is given by

$$\mathbf{d}(\mathbf{p}) = \eta_1 \mathbf{d}_1^{E_u}(\mathbf{p}) + \eta_2 \mathbf{d}_2^{E_u}(\mathbf{p}). \quad (3)$$

The nematic state with  $(\eta_1, \eta_2) = \Delta(\cos \vartheta, \sin \vartheta)$  spontaneously breaks rotational symmetry, and is degenerate with respect to the angle  $\vartheta \in [0, \pi/2]$ . The broken symmetry is characterized by nematic order,  $Q \equiv (|\eta_1|^2 - |\eta_2|^2, \eta_1 \eta_2^* + \eta_1^* \eta_2)$  [12, 49]. The angle  $\vartheta$  represents the orientation of two point nodes in the  $xy$  plane (Fig. 1). Although Eq. (1) respects  $D_\infty$  symmetry, corrections to Eq. (1) from hexagonal warping of the Fermi surface pins the nematic angle  $\vartheta$  to one of three equivalent crystal axes. Another competing order allowed by Eq. (3) is the chiral state with broken time-reversal symmetry,  $(\eta_1, \eta_2) = \Delta(1, \pm i)$ . The chiral state,  $\mathbf{d}_1 \pm i \mathbf{d}_2$ , is a non-unitary state with two distinct gaps: one full gap, and another with point nodes at  $\mathbf{p} = \pm p_{Fz} \hat{z}$ .

In Fig. 1(c), we show the phase diagram of  $M_x\text{Bi}_2\text{Se}_3$  obtained from quasiclassical theory [44]. The intercalation of  $M$  atoms between the quintuple layers modifies the  $c$ -axis length of the crystal, namely, the hopping parameters along the  $z$ -axis  $(c_1, m_1, v_z)$ . This makes the Fermi pocket around the  $\Gamma$  point elongate in the  $\hat{z}$  direction. The Fermi surface indeed evolves from a closed spherical shape to a quasi-two-dimensional open cylinder as  $\mu$  increases [38, 39]. The gap structure of the nematic state changes from a point-nodal to a line-nodal structure as the Fermi surface evolves [ Fig. 1(b) ] [50]. In contrast, the

point nodes of the chiral state disappear and the fully gapped chiral state becomes thermodynamically stable when the Fermi surface is opened in the  $z$ -direction. To incorporate the Fermi surface evolution, we follow Ref. [50]: the set of parameters in Ref. [42] for  $\mu = 0.4\text{eV}$  and the half-value of  $(c_1, m_1, v_z)$  for  $\mu = 0.65\text{eV}$ . The parameters for arbitrary  $\mu$  are given by interpolating  $(c_1, m_1, v_z)$  linearly with respect to  $\mu$ . With this parametrization, the Fermi surface is opened along the  $z$ -axis for  $\mu \gtrsim 0.5\text{eV}$ . Using this set of parameters, we calculate the thermodynamic potential within the quasiclassical theory, which is valid for  $\Delta \ll \mu$ . Figure 1 shows the **first-order** phase boundary between the nematic and chiral ground states near  $\mu_c \sim 0.7\text{eV}$ . Thus, the nematic-to-chiral phase transition can be driven by Fermi surface evolution, as well as the exchange coupling to magnetic moments of dopant atoms [51, 52] and the thickness of materials [53, 54]. **Note that the result obtained above is based on a simple interpolation of the Fermi surface evolution. The phase boundary may be shifted in real materials.**

*Nematicity and chiral Higgs mode.* Consider the nematic state,  $\mathbf{d}(\mathbf{p}_F) = \Delta(T, \mu) \mathbf{d}_1^{E_u}(\mathbf{p}_F)$ , corresponding to  $\vartheta = 0$ . The fluctuations in the  $E_u$  ground state,  $\delta \mathbf{d}(\mathbf{p}_F, \mathbf{Q}, t) \equiv \mathbf{d}(\mathbf{p}_F, \mathbf{Q}, t) - \Delta \mathbf{d}_1^{E_u}(\mathbf{p}_F)$ , decompose into the  $(\Gamma, j)$  eigenmodes

$$\delta \mathbf{d}_\mu^C(\mathbf{p}_F, \mathbf{Q}, t) = \sum_{\Gamma}^{\text{odd}} \sum_{j=1}^{n_\Gamma} \mathcal{D}_{\Gamma, j}^C(\mathbf{Q}, t) \mathbf{d}_{\mu, j}^\Gamma(\mathbf{p}_F), \quad (4)$$

where  $\mathbf{Q}$  is the center-of-mass momentum of Cooper pairs. In the weak-coupling limit, all the bosonic excitations are classified in terms of the parity under particle-hole conversion ( $C = \pm$ ),  $\mathcal{D}_j^C = \mathcal{D}_j + C \mathcal{D}_j^*$ . The  $A_{1u}$  and  $A_{2u}$  modes may also exist as long-lived bosons in the spectrum of the nematic state even when  $T_c > T_c^{A_{1u}}, T_c^{A_{2u}}$ . For  $\Gamma = E_u$ , there exist four collective modes. Two of these modes are fluctuations in the ground state sector,  $\mathcal{D}_{E_u, 1}^C$ , the other two modes are in the orthogonal sector  $\mathcal{D}_{E_u, 2}^C$ . The  $\mathcal{D}_{E_u, 1}^C$  modes correspond to the NG mode associated with the broken  $U(1)_N$  symmetry ( $\mathcal{D}_{E_u, 1}^-$ ), which is gapped out by the Anderson-Higgs mechanism [55, 56], and  $\mathcal{D}_{E_u, 1}^+$  corresponding to the amplitude Higgs mode with mass  $2\Delta$ .

The bosonic modes orthogonal to the ground-state sector are represented by  $\mathcal{D}_{E_u, 2}^C$ . Let us define  $\mathcal{D}_{E_u, 2}^+ = \mathcal{D}_{E_u, 2} + \mathcal{D}_{E_u, 2}^* = \Delta \delta \vartheta(t)$  and  $\mathcal{D}_{E_u, 2}^- = \mathcal{D}_{E_u, 2} - \mathcal{D}_{E_u, 2}^* = i\epsilon(t)\Delta$ , where  $\delta \vartheta, \epsilon \in \mathbb{R}$ . Thus,  $\mathcal{D}_{E_u, 2}^+$  corresponds to  $\mathbf{d}(t) = \Delta[\mathbf{d}_1^{E_u} + \delta \vartheta(t) \mathbf{d}_2^{E_u}]$ , for  $|\delta \vartheta| \ll 1$ . This is the pseudo-NG mode associated with the broken rotational symmetry, and represents fluctuations of the nematic order parameter  $Q$ . The  $\mathcal{D}_{E_u, 2}^-$  mode represents excitation of chiral Cooper pairs,  $\mathbf{d}(t) = \Delta[\mathbf{d}_1^{E_u} + i\epsilon(t) \mathbf{d}_2^{E_u}]$ . We refer to  $\mathcal{D}_{E_u, 2}^+$  and  $\mathcal{D}_{E_u, 2}^-$  as the nematicity mode and chiral Higgs mode, respectively.

Let us now consider the linear response to EM fields,  $-\frac{e}{c} \mathbf{v}_F \cdot \mathbf{A}(\mathbf{Q}, \omega)$ , where  $\mathbf{A}$  is a vector potential. The dynamical properties of the superconducting state of  $M_x\text{Bi}_2\text{Se}_3$  are governed by Bogoliubov quasiparticles (QPs) in the CB and long-lived bosonic excitations of the pair condensate. The bosonic excitations involve a coherent motion of macroscopic fractions of particles, while low-lying QPs are responsible for the dissipation and the pair-breaking channels. To incorporate the interplay between them, we utilize the quasiclassical Keldysh transport theory [57]. The fundamental quantity is the quasiclassical

Keldysh propagator for CB electrons, which contains both Bogoliubov QPs and dynamical bosonic fields, and are governed by the transport-like equation [57–59]. The linear response of the order parameter to the vector potential  $\mathbf{A}$  is obtained from the equations of motion

$$\left[\omega^2 - \mathbb{M}_{\Gamma,j}^C(\mathbf{Q}, \omega)\right] \mathcal{D}_{\Gamma,j}^C(\mathbf{Q}, \omega) = \frac{e}{c} \mathcal{Q}_\mu \zeta_{\mu\nu}^{(\Gamma,j)}(\mathbf{Q}, \omega) A_\nu, \quad (5)$$

where  $\mathbb{M}_{\Gamma,j}^-$  microscopically determines the mass and lifetime of the mode [44]. Note that particle-hole symmetry prohibits the direct coupling of the  $C = +$  nematicity mode to transverse EM fields (i.e.,  $\zeta = 0$ ). However, the  $C = +$  mode does contribute to the dynamical spin susceptibility [44]. For  $C = -$ , the coupling of the EM field to the bosonic excitations is governed by the matrix elements

$$\zeta_{\mu\nu}^{(\Gamma,j)}(\mathbf{Q}, \omega) = \Delta \frac{\langle \bar{\lambda}(\mathbf{p}_F, \mathbf{Q}) v_F^\mu v_F^\nu d_1^{(E_u)}(\mathbf{p}_F) \cdot \mathbf{d}_j^{(\Gamma)}(\mathbf{p}_F) \rangle_{\text{FS}}}{\langle \bar{\lambda}(\mathbf{p}_F, \mathbf{Q}) |d_j^{(\Gamma)}(\mathbf{p}_F)| \rangle_{\text{FS}}}, \quad (6)$$

where  $\langle \dots \rangle_{\text{FS}} \equiv \int dS_{\mathbf{p}} \dots$  is an average over the Fermi surface obtained from Eq. (1) that satisfies  $\int dS_{\mathbf{p}} = 1$ . The tensor  $v_F^\mu v_F^\nu$  determines the coupling to  $\mathbf{A}$  ( $v_F^\nu$ ) and  $\mathbf{Q}$  ( $v_F^\mu$ ), respectively, where  $v_F^\mu \equiv \partial E_{\text{CM}} / \partial p_\mu$  is the Fermi velocity of CB electrons. Hence,  $\zeta_{\mu\nu}^{(\Gamma,j)}$  in Eq. (6) determines the coupling of  $(\Gamma, j)$  bosonic modes to EM fields with  $\mathbf{A}$  and  $\mathbf{Q}$ . The generalized Tsuneto function [60], given by  $\bar{\lambda} = \int_{|d|}^{\infty} \frac{d\epsilon}{\sqrt{\epsilon^2 - |d|^2}} \frac{\tanh(\epsilon/2T)}{\epsilon^2 - \omega^2/4}$  for  $\mathbf{Q} \rightarrow \mathbf{0}$ , is real and positive below the pair-breaking edge  $\omega < |d(\mathbf{p}_F)|$ , while it has an imaginary part for  $\omega > |d(\mathbf{p}_F)|$  which contributes to the dissociation of bosonic modes into Bogoliubov QPs [44, 61].

The dispersion relations,  $\omega_{\Gamma,j}^C(\mathbf{Q})$ , are determined from Eq. (5) by solving the nonlinear equation,  $\omega^2 - \mathbb{M}_{\Gamma,j}^C(\mathbf{0}, \omega) = 0$ , which corresponds to a pole of  $\delta \mathcal{D}_{\Gamma,j}^C / \delta A_\mu$ . In Fig. 2, we plot the mass gap of the bosonic modes,  $M_{\Gamma,j}^C \equiv \omega_{\Gamma,j}^C(\mathbf{0})$ , including the chiral Higgs and nematicity modes. The parameters are the same as those in Fig. 1(c). At  $T = 0$ , the nematicity mode remains gapless irrespective of  $\mu$ . The gapless spectrum of the nematicity mode is protected by the enlarged  $D_\infty$  symmetry of Eq. (1), and it is gapped out by terms that are higher-order in  $p$ , such as the hexagonal warping energy. Figure 2(b) shows that the mass of the nematicity mode is sensitive to the splitting of  $T_c$  of the nematic  $E_u$  states.

In Fig. 2, the mass of the chiral Higgs mode decreases as  $\mu$  increases and softens at the critical value  $\mu_{\text{DI}} = 0.71$  at  $T = 0$ . The softening indicates the dynamical instability of the nematic state towards the chiral state. As shown in Fig. 1(c), the dynamical instability at  $T = 0$  takes place in the vicinity of the nematic-to-chiral phase transition  $\mu_c$ , while it deviates from  $\mu_c(T)$  with increasing  $T$ . This implies that  $\mu_c$  is the weak first-order transition in low temperatures and the softening can be indeed captured in experiments. The damping of the chirality mode is  $-\text{Im} M_{E_u,2}^- / 2\Delta_g = 0.08$  at  $\mu = 0.5 \text{ eV}$ . The chirality mode has a long lifetime for large  $\mu$  [see Fig. S3(a) in Ref. [44]]. The QP density of states due to the point nodes decreases as  $\omega^2$ , which suppresses the pair-breaking channels for the decay of the chirality mode into QPs residing around the nodal points. Figure 2 also shows that the masses of bosonic modes supported by the competing pairing channels ( $A_{1u}$  and  $A_{2u}$ ) soften and their fluctuations develop as  $\mu$  increases.

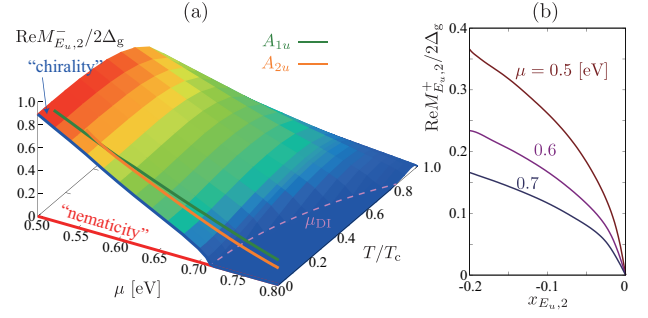


FIG. 2. (a) Mass gap of the chirality mode ( $M_{E_u,2}^-$ ), the nematicity mode ( $M_{E_u,2}^+(0, \mu)$ ), and the  $A_{1u}$  and  $A_{2u}$  modes as a function of  $\mu$ . We set  $x_{A_{1u}} = x_{A_{2u}} = -1.5$  and  $x_{E_u,2} = 0$ , where  $x_{\Gamma,j} = \ln T_c^{(\Gamma,j)} / T_c$ . The color map shows the  $T$ -dependence of the chirality mode. The dashed curve corresponds to the dynamical instability of the chirality mode at which the mass gap closes. (b) Mass gap of the nematicity mode as a function of extrinsic symmetry breaking of  $E_u$  representation measured by  $x_{E_u,2} = \ln(T_c^{(E_u,2)} / T_c)$ .

*Selection rules and EM absorption spectra.* The signatures of the bosonic spectrum and its evolution, inherent to nematic SCs, is reflected in the microwave power absorption spectrum,  $P(\omega) = \int d\mathbf{Q} \text{Re}[j(\mathbf{Q}, \omega) \cdot \mathbf{E}^*(\mathbf{Q}, \omega)]$ , that is, the Joule losses of the electric field ( $\mathbf{E}$ ) and current ( $\mathbf{j}$ ) within the penetration depth  $\Lambda = \sqrt{mc^2 / 4\pi ne^2}$  [23, 25–28]. The charge current density is obtained from the quasiclassical propagator as [44]

$$\delta j_\mu(\mathbf{Q}) = \sum_{\nu=x,y,z} \left\{ K_{\mu\nu}^{\text{QP}} - e N_F Q_\tau \sum_{\Gamma} \sum_{j=1}^{\text{odd } n_\Gamma} \zeta_{\mu\tau,j}^{(\Gamma)} \left( \frac{\delta \mathcal{D}_{\Gamma,j}^-}{\delta A_\nu} \right) \right\} A_\nu. \quad (7)$$

Equation (7) is the paramagnetic response function, including the vertex corrections from polarization of the medium by bosonic fields [23]. The term,  $K_{\mu\nu}^{\text{QP}} = -\frac{2e^2 N_F}{c} \langle [1 + \frac{(v_F^\mu \mathbf{Q})^2 (1-\lambda)}{\omega^2 - (v_F^\mu \mathbf{Q})^2}] v_F^\mu v_F^\nu \rangle_{\text{FS}}$ , where  $\lambda = |d|^2 \bar{\lambda}$ , describes the QP contribution to the dissipation via pair-breaking processes. The response,  $\delta \mathcal{D}_{\Gamma,j}^- / \delta A_\nu$ , is obtained from Eq. (5), which has a pole at the collective mode frequency  $\omega_{\Gamma,j}^-(\mathbf{Q})$  that satisfies  $\omega^2 - \mathbb{M}_{\Gamma,j}^-(\omega) = 0$ . For  $Q_{\text{vF}} \ll \Delta$  and  $v_F / \Lambda \ll \Delta$ , the power absorption spectrum is decomposed into the QP contribution and a resonance part from the collective excitations,  $P(\omega) = P^{\text{QP}}(\omega) + P^{\text{CM}}(\omega)$  [44].

Equation (6) determines the coupling of bosonic modes of the nematic state with  $\mathbf{d} = \Delta \mathbf{d}_1^{(E_u)}$  to the charge current. The  $\zeta$  function is constrained by symmetries of the equilibrium order parameter ( $\mathbf{d}_1^{(E_u)}$ ) and bosonic field ( $\mathbf{d}_j^{(\Gamma)}$ ). In addition to the chirality mode ( $\mathcal{D}_{E_u,2}^-$ ), long-lived massive bosons supported by sub-dominant pairing interactions ( $\mathcal{D}_{A_{1u}}^-$  and  $\mathcal{D}_{A_{2u}}^-$ ) are responsible for pronounced absorption peaks in the transverse EM response. In Table I, we summarize the coupling of  $\mathcal{D}_{\Gamma,j}^C$  to EM fields with the propagation vectors  $\mathbf{Q} \parallel \hat{z}$  and  $\mathbf{Q} \perp \hat{z}$  for the odd-parity ground-states ( $A_{1u}$ ,  $A_{2u}$ , and  $E_u$ ). For  $\mathbf{Q} = \hat{y}$  and  $\mathbf{A} = \hat{x}$ , the tensor  $v_F^\mu v_F^\nu$  in Eq. (6) reduces to  $v_F^x v_F^y \sim p_x p_y$ . As  $\bar{\lambda}$  is an even function on  $\mathbf{p}$ , only the chiral Higgs mode with  $\mathbf{d}_2^{(E_u)}$  couples to the transverse EM field. The selection rules for the ground-states,  $A_{1u}$  and  $A_{2u}$ , are obtained by replacing  $\mathbf{d}_1^{E_u}$  to  $\mathbf{d}^{A_{1u}}$  and  $\mathbf{d}^{A_{2u}}$  in Eq. (6), respectively. The contributions from the  $A_{1u}$  state are prohibited by the enlarged symmetry  $D_\infty$

TABLE I. Selection rules for the coupling of transverse EM waves with  $\mathbf{Q}$  to the bosonic modes,  $\mathcal{D}_{\Gamma_j}^-$  (third-to-sixth columns). The second column denotes the irreducible representations of the ground-state (G.S.) order parameter. We take  $\hat{z}$  along the (111) axis of the  $D_{3d}$  crystal.

$\mathbf{Q}$	G.S.	$\mathcal{D}_{A_{1u}}^-$	$\mathcal{D}_{A_{2u}}^-$	$\mathcal{D}_{E_{u,1}}^-$	$\mathcal{D}_{E_{u,2}}^-$
$\mathbf{Q} \parallel \hat{z}$	$A_{1u}$	—	—	—	—
	$A_{2u}$	—	—	$A \perp \hat{z}$	$A \perp \hat{z}$
	$E_{u,1}$	—	$A \perp \hat{z}$	—	—
	$E_{u,2}$	—	$A \perp \hat{z}$	—	—
$\mathbf{Q} \perp \hat{z}$	$A_{1u}$	—	—	—	—
	$A_{2u}$	—	—	$A \parallel \hat{z}$	$A \parallel \hat{z}$
	$E_{u,1}$	—	$A \parallel \hat{z}$	—	$A \perp \hat{z}$
	$E_{u,2}$	—	$A \parallel \hat{z}$	$A \perp \hat{z}$	—

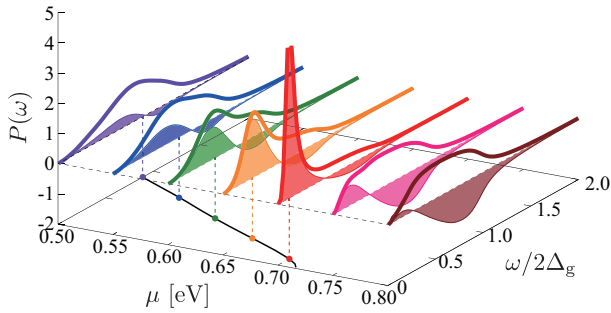


FIG. 3. Power absorption,  $P(\omega)$ , in the nematic state with the nematic angle  $\theta = 0$  for  $T = 0.05T_c$ , where we set  $\mathbf{A} \parallel \mathbf{x}$  and  $\mathbf{Q} \parallel \mathbf{y}$  and all parameters are same as those in Fig. 2. The shaded area shows the contribution of the bosonic excitations,  $P^{CM}(\omega)$ . The mass gaps of the chirality mode,  $M_{E_{u,2}}$ , are also shown.

around the small pocket of the Fermi surface. The breaking of  $D_{\infty} \rightarrow D_{3d}$  lifts this super-selection rule. In addition, the coupling of the nematicity mode to the charge current is prohibited by the particle-hole symmetry.

Figure 3 shows the power absorption,  $P(\omega)$ , and the bosonic excitation contribution,  $P^{CM}$ , for the  $E_{u,1}$  nematic ground-state at  $T = 0.05T_c$  for  $\mathbf{Q} \parallel \hat{y}$  and  $\mathbf{A} \parallel \hat{x}$ . According to the selection rules, the EM field couples to only the chiral Higgs mode,  $\mathcal{D}_{E_{u,2}}^-$ . For  $\mu = 0.5\text{eV}$ , a broad peak in the spectrum appears around  $\omega = 2\Delta_g$ . This broad peak arises primarily from the continuum of Bogoliubov QPs, i.e.,  $P^{QP}$ , and to a lesser extent the chiral Higgs mode, consistent with the large damping rate of the chiral Higgs mode shown in Fig. S3 in Ref. [44]. As  $\mu$  further increases the broad peak sharpens and shifts to lower frequencies. The pronounced peak originates from resonant absorption of the EM field by the chiral Higgs mode. The shift to lower frequency reflects the softening of the mass gap of these modes. Hence, the precursor to the dynamical instability of the nematic state to the chiral state is captured as a pronounced low-frequency peak in the EM power absorption.

Transverse EM fields with different configurations of  $\mathbf{A}(\mathbf{Q})$  couple to different bosonic modes. For instance, the EM field with  $\mathbf{A} \parallel \hat{z}$  and  $\mathbf{Q} \parallel \mathbf{x}$  couples to the chiral  $A_{2u}$  mode,  $\mathbf{d}(t) = \Delta \mathbf{d}_1^{E_u} + i\epsilon(t)\mathbf{d}^{A_{2u}}$ . Similarly to Fig. 3, a pronounced low-frequency peak appears in  $P(\omega)$  as a consequence of the resonant contribution of the chiral  $A_{2u}$  mode (see Fig. S4 in Ref. [44]).

*Signature of nematicity mode.* Finally, we note that the nematicity mode makes a significant contribution to dynamical spin susceptibility,  $\chi_{zz}(\mathbf{Q}, \omega) = \chi_{zz}^{QP}(\mathbf{Q}, \omega) + \chi_{zz}^{CM}(\mathbf{Q}, \omega)$ , where  $\chi_{zz}^{QP}(\mathbf{0}, 0)$  is the spin susceptibility of the equilibrium nematic state and  $\chi_{zz}^{CM}$  corresponds to the response of the nematicity mode (see Sec. S4 in Ref. [44]). As shown in Fig. 2(b), the mass of the nematicity mode is sensitive to  $T_c^{(E_{u,2})}/T_c^{(E_{u,1})}$ , i.e., weak symmetry-breaking perturbations to the  $D_{\infty}$ . The resulting small mass gap is detected as a pronounced peak in  $\chi_{zz}^{CM}$  at rf-frequencies resonant with the mass gap. Therefore, dynamical susceptibility measurements may provide a probe for the intrinsic mechanism of pinning the nematic order.

*Summary.* We have discovered theoretically two characteristic bosonic excitations in nematic SCs: nematicity and chirality modes. The Fermi surface evolution softens the mass gap of the chiral Higgs mode, and the mass shift reflects a distance from the nematic-to-chiral transition in low temperatures. We have also demonstrated that owing to the selection rule, only EM waves with  $\mathbf{Q} \perp \mathbf{A} \perp \hat{z}$  can directly couple to the chiral Higgs mode in nematic SCs. These results show that a pronounced peak observed in absorption measurements can be a direct probe for the chirality excitation energy from the nematic ground state.

Low-lying bosons ubiquitously exist in multi-component SCs with unconventional symmetry breaking, and the selection rule for their EM/magnetic responses is based on the generic argument with the particle-hole symmetry and gap/crystalline symmetries. Hence, EM response provides a spectroscopy of spontaneously broken symmetries and sub-dominant pairing interactions in the broad family of nematic SCs [62–64] and unconventional SCs.

This work was supported by a Grant-in-Aid for Scientific Research on Innovative Areas “Topological Materials Science” (Grants No. JP15H05852, No. JP15H05855, and No. JP15K21717) and “J-Physics” (JP18H04318) and JSPS KAKENHI (Grant No. JP16K05448 and No. JP17K05517). The research of J.A.S. was supported by the National Science Foundation Grant DMR-1508730, and in part by the Aspen Center for Physics, which is supported by National Science Foundation grant PHY-1607611.

\* mizushima@mp.es.osaka-u.ac.jp

- [1] K. Matano, M. Kriener, K. Segawa, Y. Ando, and G.-q. Zheng, *Spin-rotation symmetry breaking in the superconducting state of  $\text{Cu}_x\text{Bi}_2\text{Se}_3$* , *Nat. Phys.* **12**, 852 (2016).
- [2] S. Yonezawa, K. Tajiri, S. Nakata, Y. Nagai, Z. Wang, K. Segawa, Y. Ando, and Y. Maeno, *Thermodynamic evidence for nematic superconductivity in  $\text{Cu}_x\text{Bi}_2\text{Se}_3$* , *Nat. Phys.* **13**, 123 (2016).
- [3] Y. Pan, A. M. Nikitin, G. K. Araizi, Y. K. Huang, Y. Matsushita, T. Naka, and A. de Visser, *Rotational symmetry breaking in the topological superconductor  $\text{Sr}_x\text{Bi}_2\text{Se}_3$  probed by upper-critical field experiments*, *Sci. Rep.* **6**, 28632 (2016).
- [4] A. M. Nikitin, Y. Pan, Y. K. Huang, T. Naka, and A. de Visser, *High-pressure study of the basal-plane anisotropy of the upper critical field of the topological superconductor  $\text{Sr}_x\text{Bi}_2\text{Se}_3$* , *Phys. Rev. B* **94**, 144516 (2016).
- [5] T. Asaba, B. J. Lawson, C. Tinsman, L. Chen, P. Corbae,

- G. Li, Y. Qiu, Y. S. Hor, L. Fu, and L. Li, *Rotational Symmetry Breaking in a Trigonal Superconductor Nb-doped  $\text{Bi}_2\text{Se}_3$* , *Phys. Rev. X* **7**, 011009 (2017).
- [6] J. Shen, W.-Y. He, N. F. Q. Yuan, Z. Huang, C.-w. Cho, S. H. Lee, Y. S. Hor, K. T. Law, and R. Lortz, *Nematic topological superconducting phase in Nb-doped  $\text{Bi}_2\text{Se}_3$* , *npj Quantum Materials* **2**, 59 (2017).
- [7] G. Du, Y. Li, J. Schneeloch, R. D. Zhong, G. Gu, H. Yang, H. Lin, and H.-H. Wen, *Superconductivity with two-fold symmetry in topological superconductor  $\text{Sr}_x\text{Bi}_2\text{Se}_3$* , *Science China Physics, Mechanics & Astronomy* **60**, 037411 (2017).
- [8] M. P. Smylie, K. Willa, H. Claus, A. Snezhko, I. Martin, W.-K. Kwok, Y. Qiu, Y. S. Hor, E. Bokari, P. Niraula, A. Kayani, V. Mishra, and U. Welp, *Robust odd-parity superconductivity in the doped topological insulator  $\text{Nb}_x\text{Bi}_2\text{Se}_3$* , *Phys. Rev. B* **96**, 115145 (2017).
- [9] M. P. Smylie, K. Willa, H. Claus, A. E. Koshelev, K. W. Song, W.-K. Kwok, Z. Islam, G. D. Gu, J. A. Schneeloch, R. D. Zhong, and U. Welp, *Superconducting and normal-state anisotropy of the doped topological insulator  $\text{Sr}_{0.1}\text{Bi}_2\text{Se}_3$* , *Sci. Rep.* **8**, 7666 (2018).
- [10] A. Y. Kuntsevicha, M. Bryzgalova, V. Prudkogliada, V. Martovitskiia, Y. Selivanova, and E. Chizhevskii, *Revealing the intrinsic anisotropy of superconducting  $\text{Sr}_x\text{Bi}_2\text{Se}_3$* , arXiv:1801.09287 (2018).
- [11] K. Willa, R. Willa, K. W. Song, G. D. Gu, J. A. Schneeloch, R. Zhong, A. E. Koshelev, W.-K. Kwok, and U. Welp, *Nanocalorimetric Evidence for Nematic Superconductivity in the Doped Topological Insulator  $\text{Sr}_{0.1}\text{Bi}_2\text{Se}_3$* , arXiv:1807.11136 (2018).
- [12] L. Fu, *Odd-parity topological superconductor with nematic order: Application to  $\text{Cu}_x\text{Bi}_2\text{Se}_3$* , *Phys. Rev. B* **90**, 100509 (2014).
- [13] M. Sato, *Topological odd-parity superconductors*, *Phys. Rev. B* **81**, 220504 (2010).
- [14] L. Fu and E. Berg, *Odd-Parity Topological Superconductors: Theory and Application to  $\text{Cu}_x\text{Bi}_2\text{Se}_3$* , *Phys. Rev. Lett.* **105**, 097001 (2010).
- [15] S. Sasaki, M. Kriener, K. Segawa, K. Yada, Y. Tanaka, M. Sato, and Y. Ando, *Topological Superconductivity in  $\text{Cu}_x\text{Bi}_2\text{Se}_3$* , *Phys. Rev. Lett.* **107**, 217001 (2011).
- [16] A. Yamakage, K. Yada, M. Sato, and Y. Tanaka, *Theory of tunneling conductance and surface-state transition in superconducting topological insulators*, *Phys. Rev. B* **85**, 180509 (2012).
- [17] L. Hao and T. K. Lee, *Surface spectral function in the superconducting state of a topological insulator*, *Phys. Rev. B* **83**, 134516 (2011).
- [18] T. H. Hsieh and L. Fu, *Majorana Fermions and Exotic Surface Andreev Bound States in Topological Superconductors: Application to  $\text{Cu}_x\text{Bi}_2\text{Se}_3$* , *Phys. Rev. Lett.* **108**, 107005 (2012).
- [19] S.-K. Yip, *Models of superconducting  $\text{Cu}_x\text{Bi}_2\text{Se}_3$ : Single- versus two-band description*, *Phys. Rev. B* **87**, 104505 (2013).
- [20] T. Mizushima, A. Yamakage, M. Sato, and Y. Tanaka, *Dirac-fermion-induced parity mixing in superconducting topological insulators*, *Phys. Rev. B* **90**, 184516 (2014).
- [21] S. Sasaki and T. Mizushima, *Superconducting doped topological materials*, *Physica C* **514**, 206 (2015).
- [22] L. D. Landau and E. M. Lifshitz, *Quantum Mechanics*, Vol. 5 (Pergamon, New York, 1958) Chap. 8.
- [23] P. J. Hirschfeld, P. Wölfle, J. A. Sauls, D. Einzel, and W. O. Putikka, *Electromagnetic absorption in anisotropic superconductors*, *Phys. Rev. B* **40**, 6695 (1989).
- [24] P. J. Hirschfeld, W. O. Putikka, and P. Wölfle, *Electromagnetic power absorption by collective modes in unconventional superconductors*, *Phys. Rev. Lett.* **69**, 1447 (1992).
- [25] S. K. Yip and J. A. Sauls, *Circular dichroism and birefringence in unconventional superconductors*, *J. Low Temp. Phys.* **86**, 257 (1992).
- [26] J. A. Sauls, H. Wu, and S.-B. Chung, *Anisotropy and strong-coupling effects on the collective mode spectrum of chiral superconductors: application to  $\text{Sr}_2\text{RuO}_4$* , *Front. Phys.* **3**, 36 (2015).
- [27] H. Wu and J. A. Sauls, *Collective mode spectrum and transverse electromagnetic wave response in anisotropic  $p$ -wave model for unconventional chiral superconductors*, to be submitted (2018).
- [28] H. Wu, *Excitations in Topological Superfluids and Superconductors*, Ph. D. thesis, Northwestern University (2017).
- [29] R. Roy and C. Kallin, *Collective modes and electromagnetic response of a chiral superconductor*, *Phys. Rev. B* **77**, 174513 (2008).
- [30] S. Higashitani and K. Nagai, *Electromagnetic response of a  $k_x \pm ik_y$  superconductor: Effect of order-parameter collective modes*, *Phys. Rev. B* **62**, 3042 (2000).
- [31] M. Miura, S. Higashitani, and K. Nagai, *Effect of Order Parameter Collective Mode on Electronic Raman Spectra of Spin-Triplet Superconductor  $\text{Sr}_2\text{RuO}_4$* , *J. Phys. Soc. Jpn.* **76**, 034710 (2007).
- [32] D. S. Hirashima, *Dynamical Spin Susceptibilities in the Superconducting Phase of  $\text{Sr}_2\text{RuO}_4$* , *J. Phys. Soc. Jpn.* **76**, 034701 (2007).
- [33] H. Monien, K. Scharnberg, L. Tewordt, and N. Schopohl, *Effects of spin-orbit interaction and crystal fields on superconducting- $p$ -wave pair states and their collective excitations in cubic systems*, *J. Low Temp. Phys.* **65**, 13 (1986).
- [34] D. Fay and L. Tewordt, *Collective order-parameter modes for hypothetical  $p$ -wave superconducting states in  $\text{Sr}_2\text{RuO}_4$* , *Phys. Rev. B* **62**, 4036 (2000).
- [35] S. Maiti and P. J. Hirschfeld, *Collective modes in superconductors with competing  $s$ - and  $d$ -wave interactions*, *Phys. Rev. B* **92**, 094506 (2015).
- [36] N. Bittner, D. Einzel, L. Klam, and D. Manske, *Leggett Modes and the Anderson-Higgs Mechanism in Superconductors without Inversion Symmetry*, *Phys. Rev. Lett.* **115**, 227002 (2015).
- [37] R. M. Lutchyn, P. Nagornykh, and V. M. Yakovenko, *Gauge-invariant electromagnetic response of a chiral  $p_x + ip_y$  superconductor*, *Phys. Rev. B* **77**, 144516 (2008).
- [38] E. Lahoud, E. Maniv, M. S. Petrushevsky, M. Naamneh, A. Ribak, S. Wiedmann, L. Petaccia, Z. Salman, K. B. Chashka, Y. Dagan, and A. Kanigel, *Evolution of the Fermi surface of a doped topological insulator with carrier concentration*, *Phys. Rev. B* **88**, 195107 (2013).
- [39] B. J. Lawson, G. Li, F. Yu, T. Asaba, C. Tinsman, T. Gao, W. Wang, Y. S. Hor, and L. Li, *Quantum oscillations in  $\text{Cu}_x\text{Bi}_2\text{Se}_3$  in high magnetic fields*, *Phys. Rev. B* **90**, 195141 (2014).
- [40] H. Zhang, X.-L. Qi, X. Dai, Z. Fang, and S.-C. Zhang, *Topological insulators in  $\text{Bi}_2\text{Se}_3$ ,  $\text{Bi}_2\text{Te}_3$  and  $\text{Sb}_2\text{Te}_3$  with a single Dirac cone on the surface*, *Nat. Phys.* **5**, 438 (2009).
- [41] C.-X. Liu, X.-L. Qi, H. Zhang, X. Dai, Z. Fang, and S.-C. Zhang, *Model Hamiltonian for topological insulators*, *Phys. Rev. B* **82**, 045122 (2010).
- [42] T. Hashimoto, K. Yada, A. Yamakage, M. Sato, and Y. Tanaka, *Bulk Electronic State of Superconducting Topological Insulator*, *J. Phys. Soc. Jpn.* **82**, 044704 (2013).
- [43] L. Hao, G.-L. Wang, T.-K. Lee, J. Wang, W.-F. Tsai, and Y.-H. Yang, *Anisotropic spin-singlet pairings in  $\text{Cu}_x\text{Bi}_2\text{Se}_3$  and  $\text{Bi}_2\text{Te}_3$* , *Phys. Rev. B* **89**, 214505 (2014).
- [44] See Supplemental Material [url] for quasiclassical Keldysh theory and time-dependent Ginzburg-Landau theory, which includes Refs. [45-47].
- [45] D. Rainer and J. A. Sauls, *Strong-Coupling Theory of Superconductivity*, in *Superconductivity: From Basic Physics to New Developments*, edited by P. N. Butcher and Y. Lu (World Scientific, Singapore, 1995) p. 45-78, arXiv:1809.05264.
- [46] T. Mizushima and J. A. Sauls, *Bosonic Surface States and Acoustic Spectroscopy of Confined Superfluid  $^3\text{He-B}$* , arXiv:1801.02277 (2018).

- [47] A. B. Vorontsov and J. A. Sauls, *Thermodynamic properties of thin films of superfluid  $^3\text{He-A}$* , *Phys. Rev. B* **68**, 064508 (2003).
- [49] J. W. F. Venderbos, V. Kozii, and L. Fu, *Odd-parity superconductors with two-component order parameters: Nematic and chiral, full gap, and Majorana node*, *Phys. Rev. B* **94**, 180504 (2016).
- [49] J. W. F. Venderbos, V. Kozii, and L. Fu, *Odd-parity superconductors with two-component order parameters: Nematic and chiral, full gap, and Majorana node*, *Phys. Rev. B* **94**, 180504 (2016).
- [50] T. Hashimoto, K. Yada, A. Yamakage, M. Sato, and Y. Tanaka, *Effect of Fermi surface evolution on superconducting gap in superconducting topological insulator*, *Supercond. Sci. Technol.* **27**, 104002 (2014).
- [51] N. F. Q. Yuan, W.-Y. He, and K. T. Law, *Superconductivity-induced ferromagnetism and Weyl superconductivity in Nb-doped  $\text{Bi}_2\text{Se}_3$* , *Phys. Rev. B* **95**, 201109 (2017).
- [52] L. Chirolli, F. de Juan, and F. Guinea, *Time-reversal and rotation symmetry breaking superconductivity in Dirac materials*, *Phys. Rev. B* **95**, 201110 (2017).
- [53] A. A. Zyuzin, J. Garaud, and E. Babaev, *Nematic Skyrmions in Odd-Parity Superconductors*, *Phys. Rev. Lett.* **119**, 167001 (2017).
- [54] L. Chirolli, *Chiral superconductivity in thin films of doped  $\text{Bi}_2\text{Se}_3$* , *Phys. Rev. B* **98**, 014505 (2018).
- [55] P. W. Anderson, *Plasmons, Gauge Invariance, and Mass*, *Phys. Rev.* **130**, 439 (1963).
- [56] P. W. Higgs, *Broken Symmetries and the Masses of Gauge Bosons*, *Phys. Rev. Lett.* **13**, 508 (1964).
- [57] J. Serene and D. Rainer, *The quasiclassical approach to superfluid  $^3\text{He}$* , *Phys. Rep.* **101**, 221 (1983).
- [58] G. Eilenberger, *Transformation of Gorkov's equation for type II superconductors into transport-like equations*, *Z. Phys.* **214**, 195 (1968).
- [59] J. A. Sauls and T. Mizushima, *On the Nambu fermion-boson relations for superfluid  $^3\text{He}$* , *Phys. Rev. B* **95**, 094515 (2017).
- [60] T. Tsuneto, *Transverse Collective Excitations in Superconductors and Electromagnetic Absorption*, *Phys. Rev.* **118**, 1029 (1960).
- [61] R. H. McKenzie and J. A. Sauls, *Collective Modes and Nonlinear Acoustics in Superfluid  $^3\text{He-B}$* , in *Helium Three*, edited by W. P. Halperin and L. P. Pitaevskii (Elsevier, Amsterdam, 1990) p. 255, [arXiv:1309.6018](https://arxiv.org/abs/1309.6018).
- [62] K. Machida, *Spin Triplet Nematic Pairing Symmetry and Superconducting Double Transition in  $U_{1-x}\text{Th}_x\text{Be}_{13}$* , *J. Phys. Soc. Jpn.* **87**, 033703 (2018).
- [63] L. Andersen, Z. Wang, T. Lorenz, and Y. Ando, *Nematic superconductivity in  $\text{Cu}_{1.5}(\text{PbSe})_5(\text{Bi}_2\text{Se}_3)_6$* , *Phys. Rev. B* **98**, 220512 (2018).
- [64] K. A. M. Hasan Siddiquee, R. Munir, C. Dissanayake, P. Vaidya, C. Nickle, E. Del Barco, D. VanGennep, J. Hamlin, and Y. Nakajima, *Nematic superconductivity in topological semimetal  $\text{CaSn}_3$* , [arXiv:1901.02087](https://arxiv.org/abs/1901.02087) (2019).